Chemical Physics 54 (1980) 55–63

RADIATIVE PROPERTIES OF THE $B\,^2\Sigma^+$ AND $C\,^2\Sigma^+$ STATES IN OH AND OD

T. BERGEMAN *, P. ERMAN and M. LARSSON
Research Institute of Physics, S-104 05 Stockholm 50, Sweden

Received 27 May 1980

Radiative lifetimes and relative intensities have been measured for the B–A and C–A systems in OH and OD using the high frequency deflection technique. The measured B state lifetimes, 2–3 μs, are affected by dissociative collisional transfer in similar ways as the A state, while the C state lifetimes (around 4 ns) are consistent with the description of the C state as an ionic state. The Boltzmann distribution of the B–A emission shows two components with T = 120 and 390 K. Revised calculations of Franck–Condon factors are included.

1. Introduction

Because of its ubiquitous presence in combustion processes, in the atmosphere and in interstellar space, properties of the OH molecule are of interest for computer modeling and in the interpretation of experimental probes of numerous diverse phenomena. Also the physics of the molecule itself is interesting to study because the light mass produces a relatively open spectrum that facilitates measurements on individual rotational levels and because the relatively small number of electrons facilitates ab initio calculations.

Radiative lifetimes of excited electronic states enter directly into many of the modeling schemes and into the analysis of experimental observations of OH in its various environments, and also provide a probe of the electronic stucture. Although many investigations have been performed on the lifetimes of the lowest excited state, $A\,^2\Sigma^+$ of OH and OD (see ref. [1] and references therein), the lifetimes of the second excited state, to our knowledge, have not previously been measured, despite the fact that the OH and OD B–A transitions, although weak, are easily observable in the visible region of the spectrum in many emission sources. In this study we utilize highly dispersed fluorescence from electron bombardment of H_2O and D_2O, using the high frequency deflection technique (HFD), as described in previous reports from this laboratory [1,2], to obtain lifetimes for the B state of OH and OD. The measured B state lifetimes are longer than for the A state, which is expected since the B–A transitions occur over a region much closer to the limit, at large internuclear distance r, of a forbidden atomic transition (cf. the potential curves in fig. 1). Some points of secondary interest presented by our data are the variation of the electronic transition moment with r deduced from rela-

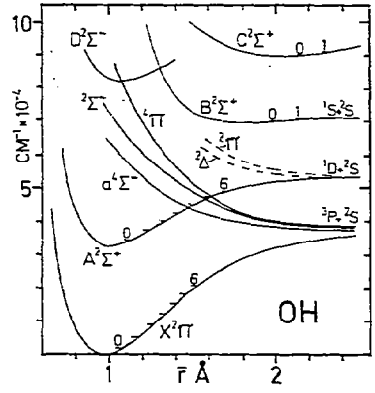

Fig. 1. Rydberg–Klein–Dunham potential curves for the $C\,^2\Sigma^+$, $B\,^2\Sigma^+$, $A\,^2\Sigma^+$ and $X\,^2\Pi$ states of OH obtained with molecular constants from ref. [9]. The RKD potentials are extended with a Morse potential curve above the highest observed vibrational level.

* Permanent address: Physics Department, State University of New York at Stony Brook, LI, NY 11794.

tive intensities of different emission bands and the evidence of dissociative collisional transfers occurring in a similar way as for the A state.

We also report a lifetime determination for the $C\,^2\Sigma^+$ state of OH and OD. After drastic discrepancies among the earlier published measurements [3–5] it is satisfying that our result for OH agrees well with the last of three published values [5], indicating that the C state lifetime data are now converging. From the point of view of molecular electronic structure, the fact that this value is rather short is of interest with respect to the suggested ionic character of the C state.

As a supplementary set of observations, we report rotational temperatures of OH and OD molecules in the B and C states as produced by electronic bombardment of H_2O and D_2O under conditions of minimal collisional transfer. The present observations present an extreme contrast to the anomalously high rotational temperatures observed in the OH $A\,^2\Sigma^+$ state under similar conditions. The rotational distributions are of interest with regard to the precursor states of the parent molecule. Recent theoretical calculations of H_2O potential curves and trajectories [6] which were so successful in explaining the A state population distribution, might now be usefully applied to those H_2O states which dissociate to the OH B and C states.

After a brief review of the experimental apparatus and measurement procedures in section 2, we present our results in section 3, some relevant Franck–Condon calculations and a discussion of the r-dependence

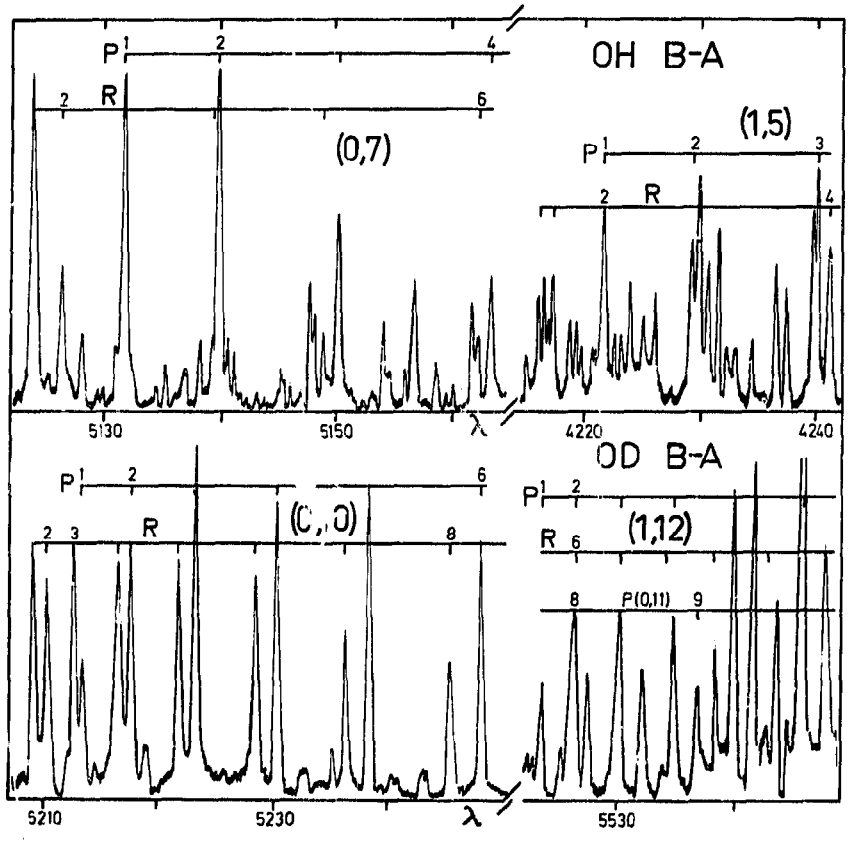

Fig. 2. Portions of OH and OD spectra following from bombardment of 75 mTorr H_2O and D_2O vapour with 20 keV, 35 mA electrons using the high frequency deflection technique involving the (0,7) and (1,5) bands of the B–A system in OH and the (0, 10) and (1,12) bands of the B–A system in OD, which were chosen for lifetime measurements.

of the B–A transition moment in section 4, and then discuss the implications, primarily for molecular electronic structure, in section 5.

2. Experimental

Figs. 2 and 3 show sections of the OH B–A, OD B–A and OH C–A bands obtained using the HFD technique [2]. The target consisted of water vapour at 75 mTorr pressure and this was bombarded with 20 keV, 35 mA electrons. The emission spectrum was observed in first order with a 2 m Czerny–Turner mounted scanning spectrometer set at 0.3 Å fwhm. The B–A spectra were recorded with a filter which removes contributions from second order lines. Spectra for the (0,8) and (0,9) bands of the B–A transition of OH and the (0,9) (0,11) bands of the B–A transition of OD were also recorded in order to determine the transition moment variation with internuclear distance.

When lifetimes are measured, the beam is rapidly pulsed in order to achieve a periodic excitation of the studied levels. The time between an exciting electron pulse and the corresponding photon pulse is measured with a time-amplitude converter (TAC) and the result is stored in a multichannel analyser. The repetition frequency chosen for a lifetime measurement is matched to the lifetime of the studied level.

The most prominent features in the OH and OD spectra were chosen for lifetime measurements, that is the (0,7), (1,5) bands for B–A, and the (0,9) and (1,9) bands for C–A of the OH molecule and the (0,10), (1,12) and (2,7) bands for B–A and the (0,10) for the C–A of the OD molecule.

Fig. 4 shows decay curves of the OD B–A (0,10) P(2) transition with D_2O at 10 mTorr as the sole target gas or with argon at 25 and 90 mTorr added. The lifetimes for the B–A transition were measured in the pressure range 1–75 mTorr yielding a zero pressure value around 2 μs. From the slope of the Stern–Volmer plot is found a quenching rate coefficient of 5 ×

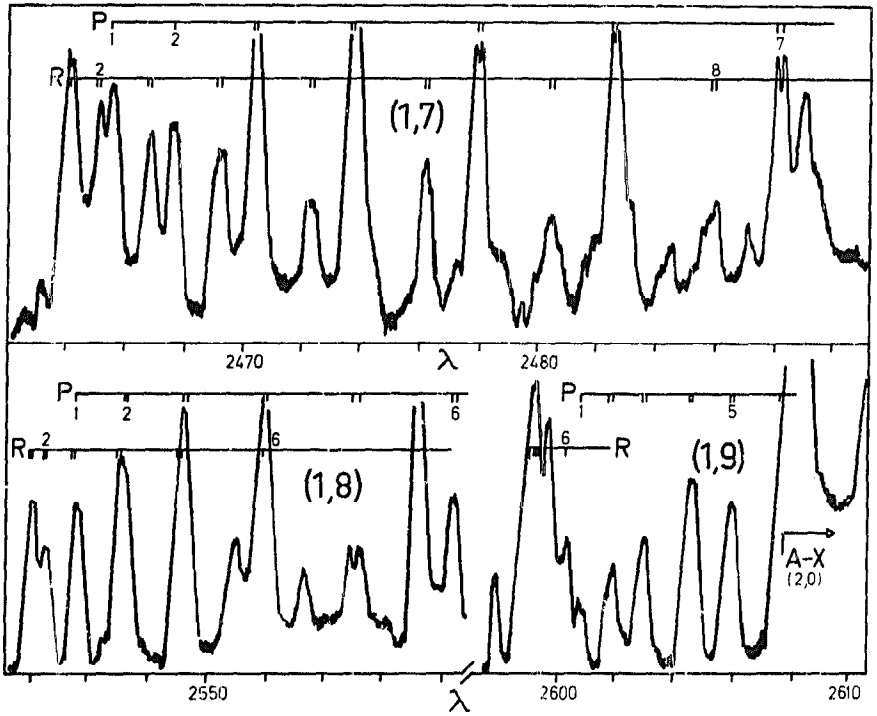

Fig. 3. The (1,7), (1,8) and (1,9) bands of the C–A transition of OH recorded under the same conditions as the spectrum shown in fig. 1.

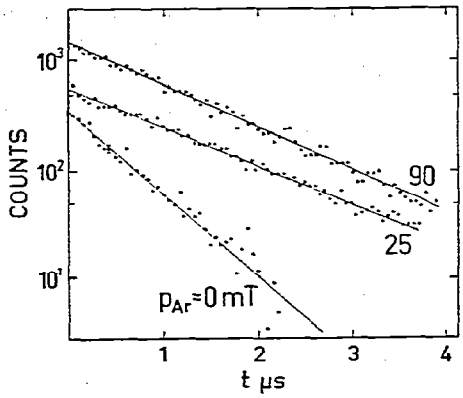

Fig. 4. Decay curve of the OD B–A (0,10) P(2) transition recorded with the HFD technique with a sweep frequency at 60 kHz. The pressure of the target gas, D_2O, was 10 mTorr, while argon at various pressures p = 0, 25 and 90 mTorr was added. With only D_2O vapour present the lifetime $\tau \approx 450$ ns. The addition of Ar causes an increase of the intensity and a lengthening of τ in a non-exponential way. This is interpreted as dissociative collisional transfers in a similar way as for the A–X system.

10^{-9} cm^3/mol s. This comparatively high value combined with a 2 μs lifetime and rather weak bands introduces a considerable uncertainty in the zero pressure values which are displayed in table 1.

The OD molecule showed a similar pressure dependence, as could be expected. In view of its short lifetime (≈3–4 ns), it was not possible to observe any pressure effects for the C state, within the pressure range used in this experiment. When such short lifetimes are measured, the decay curve is distorted by the prompt excitation peak whose half-width is about 7 ns. Consequently, the prompt peak was measured using various very short-lived transitions in neon. The radiative lifetime was then deduced from the shift of the centroid of the experimental and the prompt decay curves as described in ref. [7]. The results for the B and C states of OH and OD are summarized in table 1. The given errors include estimates of the systematic errors which greatly exceed the statistical ones.

Lifetimes were also measured at different positions in the wavelength region 1800–1900 Å of the OH spectra in order to check if the emission lines in this region had a lifetime similar to the C state. As discussed in section 5.2 this would support the theory that the observed emission arises from the $C\,^2\Sigma^+$–$X\,^2\Pi$ transition. Contrary to ref. [4], we do not find any significant difference between the lifetimes recorded in this region and the results given in table 1 for the C state of OH.

In order to compare relative intensities between different bands, the instrumental response was calibrated with a tungsten lamp. The result of these measurements will be discussed in section 4.

3. Lifetime results

In sharp contrast to the large amount of lifetime data to be found in the literature for the $A\,^2\Sigma^+$ state of OH and OD, only limited data exist for the C state (see table 1), while to our knowledge no data at all exist for the B state. As can be seen from table 1, earlier lifetime data on the C state are scattered.

The first reported lifetime of the $C\,^2\Sigma^+$ state [3] was obtained from the time-resolved emission of the (0,9) band after a pulsed discharge between elec-

Table 1
Lifetime data (ns) for the $C\,^2\Sigma^+$ and $B\,^2\Sigma^+$ states in OH and OD

	v'	$C\,^2\Sigma^+$				$B\,^2\Sigma^+$		v'	$C\,^2\Sigma^+$		$B\,^2\Sigma^+$
		a)	b)	c)	d)	a)			a)	c)	a)
OH	0	4.2 ± 0.8	3.9 ± 0.5	5.9 ± 1.2	80.0 ± 5.2	2000 ± 700	OD	0	4.5 ± 0.8	6.1 ± 1.2	2000 ± 500
	1	3.5 ± 0.8	3.7 ± 0.6	6.1 ± 1.2		3000 ± 1000		1			3000 ± 700
								2			3000 ± 1000

a) This experiment. b) Pulse radiolysis [5].
c) Phase shift technique [4]. d) Pulsed discharge [3].

trodes in water vapour. Later, a phase-shift measurement [4] yielded an order of magnitude shorter lifetime. It was also shown that OD ($C\,^2\Sigma^+$) had a similar lifetime as OH ($C\,^2\Sigma^+$). It is clear that such a short-lived emission could not have been observed in the first experiment [3]. Recently, it was confirmed [5] that the OH C state is short-lived using pulse radiolysis. As can be seen from table 1, our result for the $v' = 0,1$ levels supports that of ref. [5], and no lifetime difference is found.

No variation of the lifetime with pressure could be observed in the pressure range 10–75 mTorr used in the present experiment. This is expected in view of the quenching rate constant 1.8×10^{-9} cm^3/mol s given in ref. [5].

The results given for the $B\,^2\Sigma^+$ state in table 1 are obtained from Stern–Volmer plots extrapolated to zero-pressure. The resulting quenching rate coefficient is identical for OH and OD (5×10^{-9} cm^3/mol s) and ten times larger than the rate constant for OH $A\,^2\Sigma^+$ (cf. ref. [5] and references therein).

The change of the B–A decay curves when argon is added to the target gas (see fig. 4) probably results from dissociative collisional transfers from excited levels in the water molecules in the same way as found for the OH/OD A state (see ref. [18] and references given therein). Thus collisions between excited water molecules and argon atoms cause dissociations and an increased population of the B state levels. They give rise to a second decay component which at moderate Ar pressures [M] is observed as an apparent lengthening of the B state lifetimes, however with increasing Ar pressure the transfer feedings of the B state become relatively more important and the registered lifetime is then $\propto 1/\Sigma_i k_i[\mathrm{M}]$, where k_i are the transfer rate coefficients, i.e. it will gradually decrease with increasing [M].

The catalyzed transfer processes also yield an increased B emission intensity. Thus Ar at 60 mTorr is found to increase the B–A emission intensity a factor of five relative to the hydrogen Balmer line intensities.

4. Boltzmann distributions, transition moments and Franck–Condon factors

The intensity $I_{N',N''}$ (photons/s) of a transition $N' \to N''$ in a given band (v', v'') is given by

$$I_{N',N''} \propto N_{N'} \nu^3_{N',N''} \frac{S_{N',N''}}{2N'+1} T_{N',N''} , \tag{1}$$

with

$$T_{N',N''} = |\psi'(r)\, R_e(\bar{r})\, \psi''(r)\, \mathrm{d}r|^2 . \tag{2}$$

$N_{N'}$ denotes the population of level N', $S_{N',N''}$ the Hönl–London and R_e the electronic transition moment. In the $\bar{r}$-centroid approximation this gives the band intensity

$$I_{v',v''} \propto N_{v',v''} q_{v',v''} \nu^3_{v',v''} R^2_e(\bar{r}) . \tag{3}$$

If $N_{N'}$ is given by a Boltzmann distribution, i.e. in a reasonable approximation

$$N_{N'} \propto (2N'+1) \exp[-(hcB/kT) N'(N'+1)] \tag{4}$$

and the Franck–Condon factor q, and R_e are roughly constant within a band (it follows below that these assumptions are justified), it follows from (1), (2) and (4) that a plot of $\ln(I_{N',N''}/S_{N',N''}\nu^3_{N',N''})$ versus $N'(N'+1)$ yields a linear function whose slope gives the rotational temperature T. From such a plot up to $N' = 5$ for the B–A system in OH we find that

$$T(\mathrm{OH, B}) = 120 \pm 50\ \mathrm{K} , \tag{5}$$

while the corresponding plot for OD (see fig. 5) which is possible to extend up to $N' = 16$ shows two different components with

$$T_1(\mathrm{OD, B}) = 120 \pm 40\ \mathrm{K} , \tag{6}$$

$$T_2(\mathrm{OD, B}) = 390 \pm 60\ \mathrm{K} . \tag{7}$$

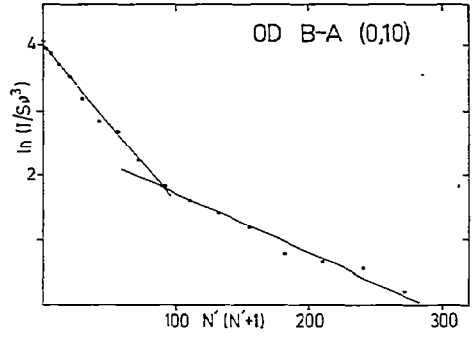

Fig. 5. Boltzmann distribution of the OD B–A (0,10) transition, according to eqs. (2), (3) and (5). Two components are clearly seen, corresponding to $T_1 = 120 \pm 40$ K and $T_2 = 390 \pm 60$ K.

Table 2
Franck–Condon factors (upper values) and r-centroids (Å) (lower values) for the OH and OD $B^2\Sigma^+$–$A^2\Sigma^+$ and $C^2\Sigma^+$–$A^2\Sigma^+$ transitions calculated with the Rydberg–Klein–Dunham method

	v'	v''													
		0	1	2	3	4	5	6	7	8	9	10	11	12	13
OH	0	5.27 – 8	2.88 – 5	6.74 – 5	8.96 – 4	7.53 – 3	4.17 – 2	1.53 – 1	3.49 – 1	3.78 – 1	6.21 – 2				
B–A		1.39	1.43	1.47	1.52	1.58	1.65	1.73	1.83	1.98	2.33				
	1	1.21 – 7	6.09 – 6	1.29 – 4	1.50 – 3	1.04 – 2	4.28 – 2	9.21 – 2	5.37 – 2	5.16 – 2	6.27 – 1				
		1.38	1.42	1.46	1.51	1.56	1.62	1.68	1.71	2.14	2.23				
OH	0	5.37 – 11	3.97 – 9	1.45 – 7	3.49 – 6	6.33 – 5	9.21 – 4	1.09 – 2	9.44 – 2	4.47 – 1	3.83 – 1				
C–A		1.42	1.48	1.54	1.60	1.67	1.74	1.82	1.91	2.01	2.17				
	1	1.28 – 9	7.91 – 8	2.34 – 6	4.38 – 5	5.75 – 4	5.52 – 3	3.72 – 1	1.37 – 1	7.90 – 2	3.09 – 1				
		1.40	1.45	1.51	1.57	1.63	1.69	1.76	1.82	1.76	2.22				
	2	1.57 – 8	8.27 – 7	2.03 – 5	3.00 – 4	2.93 – 3	1.90 – 2	7.47 – 2	1.23 – 1	8.45 – 2	1.53 – 5				
		1.39	1.43	1.48	1.54	1.59	1.65	1.72	1.77	1.87	4.11				
	3	6.73 – 8	3.16 – 6	6.71 – 5	8.38 – 4	6.50 – 3	3.09 – 2	7.72 – 2	5.48 – 2	6.29 – 3	6.68 – 2				
		1.37	1.42	1.47	1.52	1.57	1.63	1.68	1.73	1.88	2.34				
OD	0	2.64 – 10	1.40 – 8	4.30 – 7	7.84 – 6	9.51 – 5	8.15 – 4	5.11 – 3	2.38 – 2	8.20 – 2	2.05 – 1	3.36 – 1	2.86 – 1	6.07 – 2	7.90 – 4
B–A		1.37	1.40	1.43	1.47	1.50	1.54	1.59	1.64	1.70	1.77	1.85	1.97	2.20	1.29
	1	9.52 – 10	6.13 – 8	1.75 – 6	2.90 – 5	3.14 – 4	2.32 – 3	1.19 – 2	4.18 – 2	9.31 – 2	1.05 – 1	1.53 – 2	1.15 – 1	4.94 – 1	1.00 – 1
		1.37	1.39	1.42	1.46	1.49	1.53	1.57	1.62	1.67	1.72	1.68	2.00	2.11	2.46
	2	9.60 – 10	5.94 – 8	1.61 – 6	2.53 – 5	2.55 – 4	1.71 – 3	7.72 – 3	2.25 – 2	3.69 – 2	2.10 – 2	1.62 – 3	4.96 – 2	2.45 – 3	5.13 – 1
		1.36	1.39	1.42	1.45	1.48	1.52	1.56	1.60	1.65	1.68	1.96	1.85	3.28	2.37
OD	0	1.56 – 16	2.86 – 14	2.50 – 12	1.38 – 10	5.38 – 9	1.57 – 7	3.57 – 6	6.43 – 5	9.07 – 4	9.89 – 3	7.60 – 2	3.36 – 1	5.02 – 1	1.01 – 2
C–A		1.50	1.53	1.56	1.60	1.63	1.67	1.71	1.76	1.81	1.86	1.92	2.00	2.10	2.68
	1	2.80 – 15	4.71 – 13	3.73 – 11	1.83 – 9	6.25 – 8	1.56 – 6	2.95 – 5	4.20 – 4	4.37 – 3	3.11 – 2	1.21 – 1	1.24 – 1	7.92 – 2	3.97 – 1
		1.49	1.52	1.55	1.58	1.62	1.65	1.69	1.73	1.77	1.81	1.85	1.85	2.26	2.21

In view of the short N'-range, spectral overlaps and a high emission background, it is difficult to make more accurate estimates for the C state but it seems that T(OH, OD, C) is in the range 100–200 K.

From the $N' \to 0$ extrapolations of the Boltzmann plots, we obtain a measure of the band intensities $I_{v',v''}$ for a sequence of bands originating from a common upper level v' and, as follows from ref. [3], plotted as a function

$$(I_{v',v''}/q_{v',v''}\nu^3_{v',v''})^{1/2} \text{ versus } \bar{r}\,. \qquad (8)$$

This should include the relative variation of R_e with $\bar{r}$. The absolute variations for the B–A and C–A systems are not possible to deduce, since the branchings to the ground state are unknown.

In order to extract relevant information from the relative intensity measurements, more accurate Franck–Condon factors and r-centroids than hitherto available are needed. We have used Rydberg–Klein–Dunham potential curves [8] to calculate these quantities and the results are listed in table 2. The construction of the potential curves is based on molecular constants from ref. [9]. The results given in table 2 differ from earlier calculations [10], particularly for the C–A transition of OH. This is mainly due to an earlier error in the vibrational numbering of the C state, later corrected in ref. [9].

Fig. 6 shows a plot of eq. (8) for the B–A transition of OH and OD. Since the $B\,^2\Sigma^+$ states dissociate into $O(^1S) + H(^2S)$ (see fig. 1) and the $O(^1S) \to O(^3P)$ transition is forbidden, the result shown in fig. 6 is the expected one. The small difference between OH and OD is probably not significant, but rather due to errors in the intensity measurements. As compared to OH, the intensity measurements for OD are considered to be more reliable in view of the larger number of measured lines. There is also a possibility that the intensity of the (0,8) band is overestimated due to underlying lines from H_2O^+. However, lines that are known to be overlapped by H_2O^+ lines [9,11] were excluded from the intensity determination.

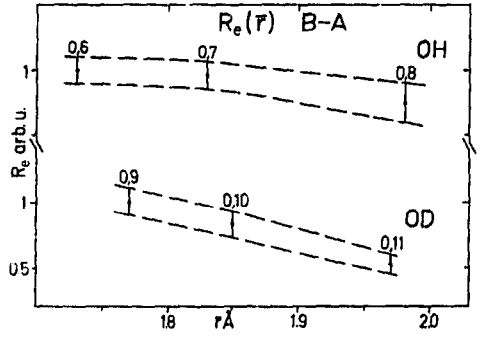

Fig. 6. The electronic transition moment R_e of the OH and OD B–A transitions as deduced from measured relative intensities and calculated Franck–Condon factors and r-centroids. R_e is expressed in arbitrary units, since no determination of the absolute transition moment is possible in view of unknown branchings to the ground state.

The result shown in fig. 6 agrees reasonably well with the earlier determination of the transition moment variation [10], also based on relative intensity measurements.

For the C–A transition the uncertainties in the band intensity measurements are larger than for B–A, due to the above-mentioned cause. However, the intensities roughly follow the Franck–Condon factors, which indicate a constant transition moment for both the OH and OD C–A transition to within 20% for $\bar{r} = 1.8$–2.2 Å.

5. Discussion

5.1. B state lifetimes

Compared to the A state, the B state lifetime is almost three times longer which is not unexpected since the B state consists of a very weakly bound hydrogen atom attached to an $O\,^1S$ atom, for which the radiative decays to ^3P and ^1D are highly forbidden at the atomic limit. Thus, although no definite answer can be given, in view of the long lifetimes, it is unlikely that the B state levels are subjected to any substantial predissociation effects. In fig. 1 we have indicated that, according to the calculations [14] the second $^2\Pi$ state is closest to the $B\,^2\Sigma^+$ potential curve, but is not believed to cross it and cause strong predissociations.

5.2. C state lifetimes

The relatively short C state lifetimes, 4.2 and 3.5 ns for the $v' = 0$ and 1 levels from our observations, 3.9 and 3.7 ns for $v = 0$ and 1 from the result of ref. [5], are consistent with the description of the C state

as an ionic state (O^-H^+) proposed in refs. [9,15] and as confirmed in CI calculations [14]. An ionic wavefunction would imply not only a large dipole moment for the C state (as yet unobserved) but also relatively large oscillator strengths for transitions to valence states as the electronic density shifts toward the H atom.

The contribution to the total decay rate from predissociation is unknown but is likely to be small for the levels we have observed. From the absence of emission bands from $v = 2$ of the C state, it does appear that a repulsive curve crosses the C state slightly above the $v = 1$ level, but the coupling is not terribly strong, since $v = 3$ is again observed in emission. It is reported that emission from $v = 1$ breaks off sharply at $N = 9$ [9], presumably due to coupling with the same repulsive state that depopulates $v = 2$. Judging, for example, from lifetime measurements of predissociation in the OH A state [1,12], the onset of predissociation tends to occur abruptly with N, so if this comparison is valid the levels we have observed, $N = 1$–3, are not likely to be strongly affected. The fact that we observe approximately the same lifetime in $v = 0$ as in $v = 1$ of the OH C state reinforces the argument that predissociation in these levels is slight, although there may be some background effect, as proposed for the B state noted above.

One of the outstanding spectroscopic problems for OH is the assignment of the dense spectral region from 1750 to 1900 Å which has tentatively been attributed to transitions from the C state to high levels of $X^2\Pi$ [10,16,17]. The fact that we observe approximately the same upper state lifetimes at four points in this spectral region as for the C–A transitions, to within 50%, reinforces this assignment. Similar but less consistent observations were reported by the phase-shift measurements [4] yielding lifetimes of ≈6 ns for the C–A bands and ≈2 ns at several points between 1800 and 1900 Å. Of course the possibility of other transitions in this region (cf. ref. [14]) is not excluded. It may be that the upper state of another band system may coincidentally have a lifetime similar to or shorter than the C state, or, at the wavelengths sampled, lines of the second system happen to have negligible intensity. Only a rotational analysis of this dense spectral region will settle these questions.

5.3. Rotational temperatures

Incidental to the lifetime measurements, the apparent rotational temperature observed in the OH emission spectrum produced by 20 keV electron bombardment in our apparatus provides useful information of the process of formation of OH fragments in various electron states from the parent molecules H_2O or D_2O. Present observations may be compared with numerous studies of the rotational distribution in the $A^2\Sigma^+$ state. For example, a recent investigation from this laboratory [18] reported that the very low N levels of the A state exhibited a temperature in the vicinity of room temperature, but above about $N \approx 10$, the distribution was characterized by a temperature of about 19 000 K. Such high temperatures have been interpreted with the help of computed H_2O potential surfaces [6] as being associated with the A^1B_1 H_2O state which falls sharply in energy with increasing H–O–H bond angle as one O–H bond breaks. Thus as the H_2O molecule dissociates, the OH fragment experiences a sharp torque.

By contrast, our observations of the rotational distribution in the OH and OD B states reveal an anomalously *low* effective rotational temperature (for low N levels). The results cited in section 4 eq. (6) and shown in fig. 5 for OD give, for rotational energies <240 cm^{-1} the effective temperature $T \approx 120$ K, while higher-lying levels are consistent with $T \approx 400$ K. Previously [19], with an entirely different type of source, using microwave excitation, a very similar two-component rotational distribution was reported for the B state of OH. The two temperatures reported [19] were 130 K and 350 K, with a break point at about 200 cm^{-1} rotational energy, or just slightly lower than that shown in our fig. 5. Such similar observations from different sources suggest that the basic process of formation of the B state from H_2O/D_2O is responsible for the two temperature components. Since neither component of the B state has an elevated temperature, we conclude that the H_2O/D_2O surfaces yielding B state fragments do not vary sharply with bond angle. The hydrogen or deuterium atom is ejected without giving a torque to the OH/OD fragment. Obviously ab initio calculations are needed to clarify the situation and to explain the origin of the two-component distribution. To our knowledge there are no published complete surfaces

for electronic states of H_2O which dissociate to OH $B^2\Sigma^+$, although one such state and its dependence on bond distance is given in ref. [6].

References

[1] J. Brzozowski, P. Erman and M. Lyyra, Phys. Scripta 17 (1978) 507.
[2] P. Erman, Phys. Scripta 11 (1975) 65.
[3] F. Remy, Spectry. Letters 4 (1971) 319.
[4] W.H. Smith and G. Stella, J. Chem. Phys. 63 (1975) 2395.
[5] T.I. Quickenden, J.A. Irvin and D.F. Sangster, J. Chem. Phys. 69 (1978) 4395.
[6] S. Tsurubuchi, Chem. Phys. 10 (1975) 335.
[7] R.E. Bell, in: Alpha-, beta- and gamma-ray spectroscopy, ed. K. Siegbahn (North-Holland, Amsterdam, 1965) ch. 17.
[8] N. Elander, Thesis, Stockholm (1977).
[9] C. Carlone and F.W. Dalby, Can. J. Phys. 47 (1968) 1945.
[10] P. Felenbok, Ann. Astrophys. 26 (1963) 393.
[11] H. Lew, Can. J. Phys. 54 (1976) 2028.
[12] R.A. Sutherland and R.A. Anderson, J. Chem. Phys. 58 (1973) 1226.
[13] D. Wilcox, R. Anderson and J. Peacher, J. Opt. Soc. Am. 65 (1975) 1368.
[14] I. Easson and M.H.L. Pryce, Can. J. Phys. 51 (1973) 518.
[15] A. Michel, Z. Naturforsch. 12a (1957) 887.
[16] P. Felenbok and J. Czerny, Ann. Astr. 27 (1964) 244.
[17] B. Rosen, Données spectroscopiques relatives aux molécules diatomiques, Ed. B. Rosen (Pergamon Press, New York, 1970) p. 297.
[18] P. Erman and M. Larsson, Phys. Scripta 22 (1980) 348.
[19] J. Czerny and P. Felenbok, Ann. Astr. 31 (1968) 171.